Optimization for trapezoidal combined footings: Optimal design

Arnulfo Luévanos-Rojas[*]

Institute of Multidisciplinary Researches, Autonomous University of Coahuila,
Blvd. Revolución No, 151 Ote, CP 27000, Torreón, Coahuila, México

Abstract. This work presents a complete optimal model for trapezoidal combined footings that support a concentric load and moments around of the "X" and "Y" axes in each column to obtain the minimum area and the minimum cost. The model presented in this article considers a pressure diagram that has a linear variation (real pressure) and the equations are not limited to some cases. The classic model takes into account a concentric load and the moment around of the "X" axis (transverse axis) that is applied due to each column, i.e., the resultant force is located at the geometric center of the footing on the "Y" axis (longitudinal axis), and when the concentric load and moments around of the "X" and "Y" axes act on the footing is considered the uniform pressure applied on the contact surface of the footing, and it is the maximum pressure. Four numerical problems are presented to find the optimal design of a trapezoidal combined footing under a concentric load and moments around of the "X" and "Y" axes due to the columns: Case 1 not limited in the direction of the Y axis; Case 2 limited in the direction of the Y axis in column 1; Case 3 limited in the direction of the Y axis in column 2; Case 4 limited in the direction of the Y axis in columns 1 an 2. The complete optimal design in terms of cost optimization for the trapezoidal combined footings can be used for the rectangular combined footings considering the uniform width of the footing in the transversal direction, and also for different reinforced concrete design codes, simply by modifying the resisting capacity equations for moment, for bending shear, and for the punching shear, according to each of the codes.

Keywords: bending shear; minimum cost; moments; optimal design; punching shear; trapezoidal combined footings

1. Introduction

The soil pressure under a footing is distributed in accordance with the soil type, the soil's relative rigidity and the foundation, and the depth of the contact between foundation and soil. Fig. 1 presents the diagrams that are valid for rigid footings. Fig. 1(a) shows the pressure distribution diagram for the footing resting on sandy soils (granular soils). Fig. 1(b) presents the pressure distribution diagram for the footing resting on clayey soils (cohesive soils). Thus, it is assumed for simplicity that the footing is a perfectly rigid body, the soil is behaving elastically and the distributions of the stress and the strain are linear in the soil below the base of the footing. Therefore, the proposed design assumes that the soil pressure is distributed linearly. The distribution of soil pressure is uniform, if the footing centroid coincides with the resultant force of the loads applied on the footing (see Fig. 1(c)) (Luévanos-Rojas 2014b, 2015a, Luévanos-Rojas *et al.* 2017b).

The practice construction of a combined footing can be used for more of a column due to: 1) if the columns are located very close to each other (for example, on escalators and elevators); 2) the size of the footings can be restricted by the property line. A column located in the footing edge generates an eccentricity on the footing, but, the footing can

be attached to the footing of an inner column, and as result a combined footing is obtained.

The traditional model for the design of combined footings by rigid method considers the following: 1) The footing or foundation slab is infinitely rigid, and therefore, the deflection of the footing or foundation slab is not influenced by the pressure distribution; 2) The ground pressure distribution must be in straight line or a plane surface such way that the ground pressure centroid must located in the action line of the resultant force (longitudinal axis) of all the loads that act on foundations; 3) The minimum stress is limited to zero, because the ground cannot to support tensile stresses; 4) The maximum stress is limited to the soil allowable load capacity.

Main works of various researchers in recent years on the foundation structures or structural footings are: Guler and Celep (2005) developed the response of a rectangular plate-column system on a tensionless Winkler foundation subjected to static and dynamic loads. Wang and Kulhawy (2008) developed a design considering the construction economics and results in a foundation that has the optimal cost (minimum construction cost). Wang (2009) estimated a design that groups economic design optimization with reliability based methodologies to rationally explicate the geotechnical related uncertainties. Chen *et al.* (2011) presented a study on elastic foundations of nonlinear vibration for hybrid composite plates. Zhang *et al.* (2011) presented semi-analytical solutions for vertical and horizontal displacements, axial force, shear force and bending moment of the beam under symmetric loads resting

---

[*]Corresponding author, Ph.D.,
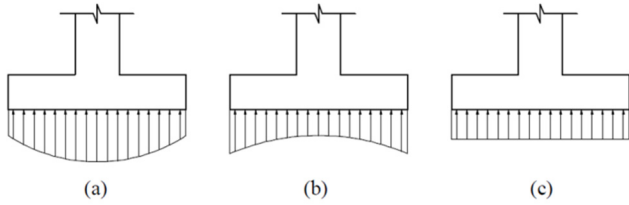E-mail: arnulfol_2007@hotmail.com

Fig. 1 Pressure distribution diagram: (a) sandy soils
(granular soils); (b) clayey soils (cohesive soils);
(c) distribution simplified

on the Winkler elastic foundation by Galerkin method.
Kalinli *et al*. (2011) proposed two different approaches to
determine the ultimate bearing capacity of shallow
foundations on granular soil, the first is an artificial neural
network (ANN) model, and the second is an improved
Meyerhof formula by a parallel ant colony optimization
algorithm, both to obtain the ultimate bearing capacity.
Smith-Pardo (2011) showed the framework based on the
performance of soil and structure systems using simplified
rocking foundation models. Shahin and Cheung (2011)
proposed the bearing capacity for strip footings by means of
stochastic design charts. Rad (2012) investigated elastic
foundations with compound loads and gradient thickness to
evaluate the static response for a circular plate of 2-D
functionally graded. Maheshwari and Khatri (2012) showed
the geosynthetic layer inclusion influence on combined
footings response on earth beds reinforced with a stone
column. Orbanich *et al*. (2012) investigated the
strenghtening and repair of concrete foundation beams whit
fiber composite materials. Basudhar *et al*. (2012) presented
the minimum cost design of a circular footing for
generalized loadings. Agrawal and Hora (2012) analyzed
the mass soil, isolated column footings, infill wall and the
building frame acting as a complete structural system under
seismic loads. Khajehzadeh *et al*. (2012) presented the
minimum cost design for shallow foundations by means of
the gravitational search algorithm. Rizwan *et al*. (2012)
showed a direct search computational procedure to obtain
the optimized design of reinforced concrete combined
footings. Luévanos-Rojas *et al*. (2013) presented a new
mathematical model for design of isolated footings of
rectangular shape. Mohamed *et al*. (2013) studied the
generalized equation of Schmertmann for shallow footings
using saturated and unsaturated sands to obtain the
settlement. Orbanich and Ortega (2013) analyzed the plates
of elastic foundation by means of finite differences method
using internal and perimeter beams supported on elastic
foundations. Al-Ansari (2013) developed an analytical
model to obtain the minimum cost for the design of
reinforced concrete rectangular isolated footings. Luévanos-
Rojas (2014a) presented a new mathematical model for
design of isolated footings of circular shape. Hassaan
(2014) studied an optimal cost design of machinery shallow
foundations resting on sand soils. Al-Ansari (2014)
presented the cost of the reinforced concrete paraboloid
footing in a plant with edge beams. Khajehzadeh *et al*.
(2014) studied an optimization technique of shallow
foundation using the gravitational search algorithm (GSA)

for the multi-objective optimization of footing. Luévanos-
Rojas (2014b) designed the combined footings of
rectangular shape to solve the problem of propriety line
using a novel model. Luévanos-Rojas (2015a) improved a
novel model for the design of combined footings with limit
on one of its sides of trapezoidal shape. Uncuoğlu *et al*.
(2015) estimated the load capacity of the square footings on
a layer of sand that overlaps with the clay. Luévanos-Rojas
(2016a) presented a comparison between two novel models
for the design of the isolated footings of rectangular and
circular type, and the results showed that the circular
footings are more economical. Yeh and Huang (2016)
estimated the effects of strengths of steel and concrete,
eccentricity and bar size on the optimization of eccentrically
loaded footings. Keawsawasvong and Ukritchon (2016)
presented a practical method for the optimal design of a
continuous footing subjected to vertical and horizontal
loads to find the minimum dimension of footing and the
minimum reinforcement steel, the method is presented in
nonlinear minimization form. Luévanos-Rojas (2016b)
developed a new model for the design of rectangular
combined boundary footings with two opposite sides
restricted. Luévanos-Rojas *et al*. (2017a) proposed a model
optimized for the design of the isolated footings that have
rectangular shape taking into account the real soil pressure.
Yeh and Huang (2017) studied the effects of the
compressive strength of concrete, yield strength of steel, the
axial load, eccentricity and steel bar dimension for the
optimization of reinforced concrete isolated footings. Khatri
et al. (2017) studied the behavior of the pressure and the
settlement of skirted footings (square and rectangular)
resting on sandy soil. Luévanos-Rojas *et al*. (2017b)
showed a comparison between two novel models for the
design of the combined footings that have trapezoidal and
rectangular shape, and the results indicated that the
trapezoidal footings are more economical. Mohebkhah
(2017) investigated the load capacity for the strip footings
on a stone masonry trench in clay. López-Chavarría *et al*.
(2017) studied an analytical model to obtain the minimum
cost design for square isolated footings based in
optimization techniques. Lins da Silva *et al*. (2017)
presented the use of the order statistics when predicting pile
foundation failure probability that study the probabilistic
moments, the mean and the variation coefficient associated
to the resistant surface. Anil *et al*. (2017) investigated
experimentally and mathematically the load capacities and
settlement profiles of six irregularly shaped footings located
on sand. Jelusic and Zlender (2018) proposed an optimal
design for footings using the multiparametric mixed integer
nonlinear programming (MINLP). Malapur *et al*. (2018)
presented a design to obtain the minimum cost of reinforced
concrete column and footings by means of genetic
algorithm based in optimization techniques. Alijani and
Bidgoli (2018) studied the vibration of concrete foundation
reinforced with SiO_2 nanoparticles resting on a soil bed.
Dezhkam and Yaghfoori (2018) analyzed the vibration of
concrete foundations resting on soil that is simulated by
means of the Winkler model taking into account consider
spring element. Luévanos-Rojas *et al*. (2018) presented a
mathematical model to find the effective depth and

reinforcing steel of T-shaped combined footings. Rawat and Mittal (2018) developed a simplified approach based on Excel solver for the design of eccentrically loaded reinforced concrete isolated footings that considers the structural requirements and economics simultaneously to find a footing with minimum cost. Velázquez-Santillán *et al.* (2018) investigated an optimal model to obtain the minimum cost design for reinforced concrete rectangular combined footings. Bensaid and Kerboua (2019) estimated the thermal stability characteristics of carbon nanotube reinforced composite beams (CNTRC) on an elastic foundation under an external uniform temperature increase load. Yáñez-Palafox *et al.* (2019) developed a mathematical model to find the effective depth and reinforcing steel for the strap combined footings. Turedi *et al.* (2019) presented an investigation on the settlement and vertical load stress analysis of the ring footings on the loose sand bed by laboratory tests and numerical analysis. López-Chavarría *et al.* (2019) proposed the minimum cost design for reinforced concrete circular isolated footings using optimization techniques. Soltani *et al.* (2019) showed a new hyperbolic shear deformation theory for the mechanical buckling analysis of advanced composite plates resting on elastic foundations. Chaudhuri and Maity (2020) presented the minimum cost of the rectangular isolated footings using GA and UPSO according to the Indian code. Alazwari *et al.* (2021) studied a comprehensive buckling response of cross-ply orientation of carbon nanotube reinforced composite (CNTRC) multilayered nanobeams with different boundary conditions. Lu and Aboutaha (2021) introduced three new strengthening systems for isolated footings: BFRP wrapping system, CFRP wrapping system, and steel jacketing system. García-Galván *et al.* (2022) showed a comparative study between trapezoidal combined footings and T-shaped combined footings. Lezgy-Nazargah *et al.* (2022) developed an analysis of shallow footings rested on tensionless foundations using a mixed finite element model. Himeur *et al.* (2022) showed the coupled effect of variable Winkler–Pasternak foundations on bending behavior of FG plates exposed to several types of loading. Gör (2022) studied the bearing capacity of shallow foundations on two-layered soil using two novel cosmology-based optimization techniques. Garay-Gallegos *et al.* (2022) presented a comparative study between the new model and the current model for T-shaped combined footings, the new model is being cheaper and safer. Kashani *et al.* (2022) presented the optimal design of reinforced concrete combined footings using five swarm intelligence algorithms: particle swarm optimization (PSO), accelerated particle swarm optimization (APSO), whale optimization algorithm (WOA), ant lion optimizer (ALO), and moth flame optimization (MFO).

The works closely related to the topic addressed in this research are: Luévanos-Rojas (2015b) developed a new mathematical model for dimensioning of the boundary trapezoidal combined footings, which presents only the equations and considers that the resultant force is placed on the X axis of the center of gravity of the area of the footing, and the moment about the X axis is 0. Pasillas-Orona *et al.* (2020) presented a model to obtain the minimum area of trapezoidal combined footings, but present two cases (Case

2: the footing is limited to a property line on the heavier load side, and Case 4: the footing is limited on the two opposite sides). Luévanos-Rojas (2015a) proposed the equations for the design of combined footings with limit on one of its sides of trapezoidal footing. Luévanos-Rojas *et al.* (2017b) showed a comparison between trapezoidal and rectangular combined footings.

According to the bibliographic review, there is not more specific paper on the subject of minimum cost design for reinforced concrete trapezoidal combined footings.

This article presents a complete optimal model for trapezoidal combined footings that support a concentric load and moments around of the "X" and "Y" axes in each column, this is presents in two parts for the four possible cases: The first part shows the minimum area and the second part presents minimum cost (thickness and reinforcing steel areas), these models consider that soil support layers are elastic and the rigid footing, which comply with the biaxial bending equation, i.e., the pressure diagram is presented in linear form, and it is obtained in function of a concentric load and two orthogonal moments around of the "X" and "Y" axes applied in each column. Four numerical problems are developed under the following considerations: 1) Without limits in the direction of the Y axis; 2) Bounded in column 1 in the direction of the Y axis; 3) Bounded in column 2 in the direction of the Y axis; 4) Bounded by their opposite sides in the direction of the Y axis.

2. Methodology

2.1 Design of trapezoidal combined footings

According to the code, the critical sections for footing that supports a column of reinforced concrete according to the construction code are (ACI 318-14): 1) For the maximum moment occurs on the column face; 2) For the bending shear occurs at a distance "*d*" from the column face; 3) For the punching shear is located on "*b_o*" (critical section perimeter that is locate at a distance "d/2"from the column face in both direction).

The general equation to obtain the stress anywhere under biaxial bending

$$q_n = \frac{P}{A} + \frac{M_x y}{I_x} + \frac{M_y x}{I_y} \tag{1}$$

where: q_n = stress generated by the ground anywhere of the footing (soil pressure), A = area in plant of the footing (contact surface on the soil), P = concentric load on the footing, M_x = moment around the "X" axis, M_y = moment around the "Y" axis, x = distance measured from the "Y" axis in the direction "X" to the point under study, y = distance measured from the "X" axis in direction "Y" to the point under study, I_y = moment of inertia around the "Y" axis and I_x = moment of inertia around the "X" axis. The moments (M_x and M_y) in the clockwise direction are positive.

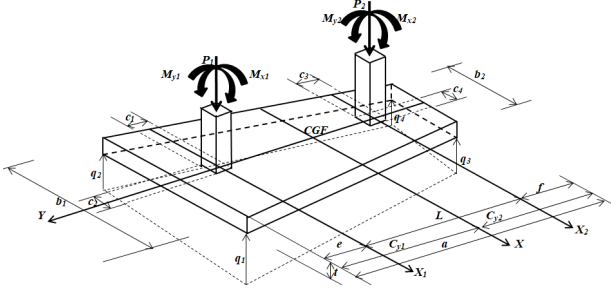Fig. 2 shows a trapezoidal combined footing that

Fig. 2 Isometric view for a trapezoidal combined footing

supports two rectangular columns of different dimensions (two columns located inside the footing) under an axial load and two orthogonal moments (biaxial bending) in each column.

The (known) constant parameters to obtain the minimum area are: P_1, M_{x1}, M_{y1}, P_2, M_{x2}, M_{y2}, R, c_1, c_2, c_3, c_4, L, q_{aa}, and the (unknown) decision variables are: A_{min}, I_x, I_y, M_{xT}, M_{yT}, a, b_1, b_2, e, f, x_1, x_2, x_3, x_4, y_1, y_2, y_3, y_4, C_{y1}, q_1, q_2, q_3, q_4.

The (known) constant parameters to find the minimum cost are: a, b_1, b_2, M_{uc}, M_{ud}, M_{ue}, M_{uf} and M_{ug}, and the parameters M_{ua}, M_{ub}, V_{uh}, V_{ui}, V_{uj}, V_{uk}, V_{ul}, V_{um}, V_{up1} and V_{up2} are presented as a function of d, and the (unknown) decision variables are: C_{min}, d, ρ_{P1}, ρ_{P2}, ρ_{yLBc}, ρ_{yLBg}, ρ_{yLTd}, ρ_{yLTe}, ρ_{yLTf}, A_{sp1}, A_{sp2}, A_{sxTB1}, A_{sxTB2}, A_{sxTB3}, A_{sxTT}, A_{syLB}, A_{syLBc}, A_{syLBg}, A_{syLT}, A_{syLTd}, A_{syLTe}, A_{syLTf}.

2.2 Minimum ground contact surface for trapezoidal combi footings

The objective function to obtain the minimum contact area on the ground "A_{min}" is

$$A_{min} = \frac{a(b_1 + b_2)}{2} \qquad (2)$$

Table 1 presents the coordinates of the pressures at each vertex of the footing.

The constraint functions to obtain the dimensions of trapezoidal combined footings are

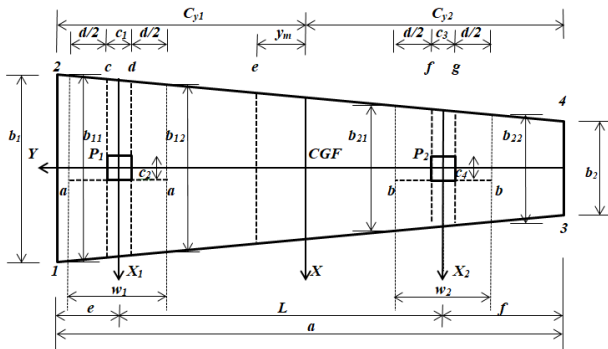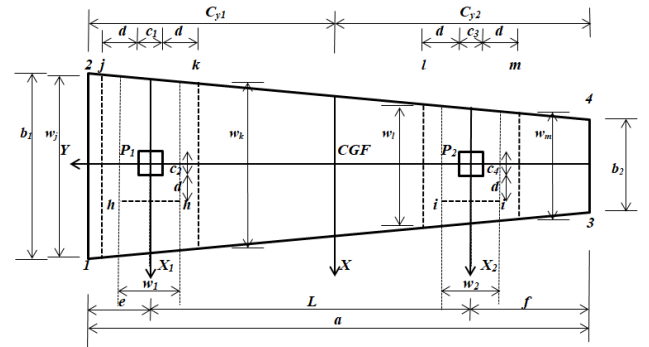$$q_n = \frac{R}{A} + \frac{M_{xT}y_n}{I_x} + \frac{M_{yT}x_n}{I_y} \qquad (3)$$

$$R = P_1 + P_2 \qquad (4)$$

$$M_{xT} = M_{x1} + M_{x2} + R(C_{y1} - e) - P_2 L \qquad (5)$$

$$M_{yT} = M_{y1} + M_{y2} \qquad (6)$$

$$C_{y1} = \frac{a(b_1 + 2b_2)}{3(b_1 + b_2)} \qquad (7)$$

$$C_{y2} = \frac{a(2b_1 + b_2)}{3(b_1 + b_2)} \qquad (8)$$

$$I_x = \frac{a^3(b_1{}^2 + 4b_1 b_2 + b_2{}^2)}{36(b_1 + b_2)} \qquad (9)$$

$$I_y = \frac{a(b_1 + b_2)(b_1{}^2 + b_2{}^2)}{48} \qquad (10)$$

$$0 \leq \begin{Bmatrix} q_1 \\ q_2 \\ q_3 \\ q_4 \end{Bmatrix} \leq q_{aa} \qquad (11)$$

$$e + L + f = a \qquad (12)$$

where: q_{aa} = Available allowable bearing capacity of the soil, R = Resultant force; M_{xT} = Resultant moment on the X axis; M_{yT} = Resultant moment on the Y axis; x_n = Distance in the X direction measured from the Y axis to the fiber under study; y_n = Distance in the Y direction measured from the X axis to the fiber under study; I_x = moment of inertia on the X axis; I_y = Moment of inertia on the Y axis.

The constraint functions for the geometric conditions are:

With both sides free

$$\frac{c_1}{2} \leq e; \frac{c_3}{2} \leq f \qquad (13)$$

With limit in column 1

$$\frac{c_1}{2} = e; \quad \frac{c_3}{2} \leq f \qquad (14)$$

With limit in column 2

Fig. 3 Moments (Critical sections)

Fig. 4 Bending shears (Critical sections)

$$\frac{c_1}{2} \le e; \quad \frac{c_3}{2} = f \tag{15}$$

With two limited opposite sides

$$\frac{c_1}{2} = e; \quad \frac{c_3}{2} = f \tag{16}$$

2.3 Minimum cost for trapezoidal combined footings

2.3.1 Equations for bending shears in one direction and moments

The critical sections for the factored moments or ultimate moments according to the ACI code for this type of footing occur in the a and b axes (axes parallel to the Y axis), and in the c, d, e, f and g axes (axes parallel to the X axis), (see Fig. 3).

The critical sections for factored bending shears or ultimate bending shears according to the ACI code for this type of footing occur in the h and i axes (axes parallel to the Y axis), and in the j, k, l, and m axes (axes parallel to the Y axis), (see Fig. 4).

The factored bending shear V_{uX1} and the factored moment M_{uY1} acting on the footing in the Y_1 axis for the interval $0 \le x_1 \le b_{11}/2$ are obtained by

$$
V_{uX_1} = \frac{M_{uy1}\left[24x_1{}^2 - 2\left(b_{11}{}^2 + b_{11}b_{12} + b_{12}{}^2\right)\right]}{(b_{11} + b_{12})\left(b_{11}{}^2 + b_{12}{}^2\right)} + \frac{P_{u1}(4x_1 - b_{11} - b_{12})}{2(b_{11} + b_{12})} \\
- \frac{3P_{u1}(w_1 - c_1)\left(b_{11}{}^2 - b_{12}{}^2\right)}{4w_1\left(b_{11}{}^2 + 4b_{11}b_{12} + b_{12}{}^2\right)} - \frac{3M_{ux1}\left(b_{11}{}^2 - b_{12}{}^2\right)}{2w_1\left(b_{11}{}^2 + 4b_{11}b_{12} + b_{12}{}^2\right)}
\tag{17}
$$

$$
M_{uY_1} = \frac{3P_{u1}(w_1 - c_1)\left(b_{11}{}^2 - b_{12}{}^2\right)(b_{11} - 2x_1)}{8w_1\left(b_{11}{}^2 + 4b_{11}b_{12} + b_{12}{}^2\right)} + \frac{P_{u1}\left[4x_1{}^2 + b_{11}b_{12}\right]}{4(b_{11} + b_{12})} - \frac{P_{u1}(b_{11} + b_{12})x_1}{2(b_{11} + b_{12})} \\
- \frac{2M_{uy1}\left(b_{11}{}^2 + b_{11}b_{12} + b_{12}{}^2\right)x_1}{(b_{11} + b_{12})\left(b_{11}{}^2 + b_{12}{}^2\right)} + \frac{M_{uy1}\left[8x_1{}^3 + b_{11}b_{12}(b_{11} + b_{12})\right]}{(b_{11} + b_{12})\left(b_{11}{}^2 + b_{12}{}^2\right)}
\tag{18}
$$

where: the study width for the bending shear and the moment in the Y_1 axis is $w_1 = c_1 + d/2$ for the edge column and for the column without limit it is $w_1 = c_1 + d$, P_{u1} is the factored axial load acting on the footing due to column 1, M_{uY1} is the factored moment acting on the footing due to column 1, the lengths of b_{11} and b_{12} are obtained as follows: $b_{11} = b_1 - (e - c_1/2 - d/2)(b_1 - b_2)/a$ (column without limit) and $b_{11} = b_1$ (edge column), and $b_{12} = b_1 - (e + c_1/2 + d/2)(b_1 - b_2)/a$.

Now, substituting $x_1 = c_2/2 + d$ into Eq. (17) the bending shear V_{uh} acting on the h axis is obtained. Substituting $x_1 = c_2/2$ into Eq. (18) the moment M_{ua} acting on the a-axis is obtained.

The factored bending shear V_{uX2} and the factored moment M_{uY2} acting on the footing in the Y_2 axis for the interval $0 \le x_2 \le b_{21}/2$ are obtained by

$$
V_{uX_2} = \frac{M_{uy2}\left[24x_2{}^2 - 2\left(b_{21}{}^2 + b_{21}b_{22} + b_{22}{}^2\right)\right]}{(b_{21} + b_{22})\left(b_{21}{}^2 + b_{22}{}^2\right)} + \frac{P_{u2}(4x_2 - b_{21} - b_{22})}{2(b_{21} + b_{22})} \\
- \frac{3P_{u2}(w_2 - c_3)\left(b_{21}{}^2 - b_{22}{}^2\right)}{4w_2\left(b_{21}{}^2 + 4b_{21}b_{22} + b_{22}{}^2\right)} - \frac{3M_{ux2}\left(b_{21}{}^2 - b_{22}{}^2\right)}{2w_2\left(b_{21}{}^2 + 4b_{21}b_{22} + b_{22}{}^2\right)}
\tag{19}
$$

$$
M_{uY_2} = \frac{3P_{u2}(w_2 - c_3)\left(b_{21}{}^2 - b_{22}{}^2\right)(b_{21} - 2x_2)}{8w_2\left(b_{21}{}^2 + 4b_{21}b_{22} + b_{22}{}^2\right)} + \frac{P_{u2}\left(4x_2{}^2 + b_{21}b_{22}\right)}{4(b_{21} + b_{22})} - \frac{P_{u2}(b_{21} + b_{22})x_2}{2(b_{21} + b_{22})} \\
- \frac{2M_{uy2}\left(b_{21}{}^2 + b_{21}b_{22} + b_{22}{}^2\right)x_2}{(b_{21} + b_{22})\left(b_{21}{}^2 + b_{22}{}^2\right)} + \frac{M_{uy2}\left[8x_2{}^3 + b_{21}b_{22}(b_{21} + b_{22})\right]}{(b_{21} + b_{22})\left(b_{21}{}^2 + b_{22}{}^2\right)}
\tag{20}
$$

where: the study width for the bending shear and the moment in the Y_2 axis is $w_2 = c_3 + d/2$ for the edge column and for the column without limit it is $w_2 = c_3 + d$, P_{u2} is the factored axial load acting on the footing due to column 2, M_{uY2} is the factored moment acting on the footing due to column 2, the lengths of b_{21} and b_{22} are obtained as follows: $b_{21} = b_1 - (L + e - c_3/2 - d/2)(b_1 - b_2)/a$, $b_{22} = b_1 - (L + e + c_3/2 + d/2)(b_1 - b_2)/a$ (column without limit) and $b_{22} = b_2$ (edge column).

Now, substituting $x_2 = c_4/2 + d$ into Eq. (19) the bending shear V_{ui} acting on the i axis is obtained. Substituting $x_2 = c_4/2$ into Eq. (20) the moment M_{ub} acting on the b-axis is obtained.

The factored bending shear V_{uY} and the factored moment M_{uX} acting on the footing in the X axis for the interval $C_{y1} - e \le y \le C_{y1}$ are given by

$$V_{uY} = -\frac{M_{uxT}[ab_1 - C_{y1}(b_1 - b_2)](C_{y1}^2 - y^2)}{2I_x a} - \frac{M_{uxT}(b_1 - b_2)(C_{y1}^3 - y^3)}{3I_x a}$$
$$-\frac{R_u[ab_1 - C_{y1}(b_1 - b_2)](C_{y1} - y)}{Aa} - \frac{R_u(b_1 - b_2)(C_{y1}^2 - y^2)}{2Aa} \tag{21}$$

$$M_{uX} = \frac{M_{uxT}(b_1 - b_2)(y^4 - 2C_{y1}y^3 + 2C_{y1}^3 y - C_{y1}^4)}{12I_x a} + \frac{M_{uxT}[b_1(2C_{y1}^3 - 3C_{y1}^2 y + y^3)]}{6I_x}$$
$$-\frac{R_u(b_1 - b_2)(C_{y1} - y)^3}{6Aa} + \frac{R_u b_1(C_{y1} - y)^2}{2A} \tag{22}$$

where: the study width for the bending shear in the j axis is $w_j = b_1 - (e - c_1/2 - d)(b_1 - b_2)/a$, and the study width for the moment in the c axis is $w_c = b_1 - (e - c_1/2)(b_1 - b_2)/a$.

Now, substituting $y = C_{y1} - e + c_1/2 + d$ into Eq. (21) the bending shear V_{uj} acting on the j-axis is obtained. Substituting $y = C_{y1} - e + c_1/2$ into Eq. (22) the moment M_{uc} acting on the c axis is obtained.

The factored bending shear V_{uY} and the factored moment M_{uX} acting on the footing in the X axis for the interval $C_{y1} - L - e \leq y \leq C_{y1} - e$ is given by

$$V_{uY} = -\frac{M_{uxT}[ab_1 - C_{y1}(b_1 - b_2)](C_{y1}^2 - y^2)}{2I_x a} - \frac{M_{uxT}(b_1 - b_2)(C_{y1}^3 - y^3)}{3I_x a}$$
$$-\frac{R_u[ab_1 - C_{y1}(b_1 - b_2)](C_{y1} - y)}{Aa} - \frac{R_u(b_1 - b_2)(C_{y1}^2 - y^2)}{2Aa} + P_{u1} \tag{23}$$

$$M_{uX} = \frac{M_{uxT}(b_1 - b_2)(y^4 - 2C_{y1}y^3 + 2C_{y1}^3 y - C_{y1}^4)}{12I_x a} + \frac{M_{uxT}[b_1(2C_{y1}^3 - 3C_{y1}^2 y + y^3)]}{6I_x}$$
$$-\frac{R_u(b_1 - b_2)(C_{y1} - y)^3}{6Aa} + \frac{R_u b_1(C_{y1} - y)^2}{2A} - P_{u1}(C_{y1} - e - y) - M_{ux1} \tag{24}$$

where: the study width for the bending shear in the k axis is $w_k = b_1 - (e + c_1/2 + d)(b_1 - b_2)/a$, and the study width for the moment in the d axis is $w_d = b_1 - (e + c_1/2)(b_1 - b_2)/a$, the study width for the bending shear in the l axis is $w_l = b_1 - (L + e - c_3/2 - d)(b_1 - b_2)/a$, and the study width for the moment in the e-axis is $w_e = b_1 - (C_{y1} - y_m)(b_1 - b_2)/a$ (y_m is the location of the maximum positive moment from the X-axis, that is, the bending shear force is equal to zero), the study width for the moment in the f axis is $w_f = b_1 - (L + e - c_3/2)(b_1 - b_2)/a$.

Now, substituting $y = C_{y1} - e - c_1/2 - d$ into Eq. (23) the bending shear V_{uk} acting on the k-axis is obtained. Substituting $y = C_{y1} - L - e + c_3/2 + d$ into Eq. (23) gives the bending shear V_{ul} acting on the l axis. Substituting $y = C_{y1} - e - c_1/2$ into Eq. (24) the moment M_{ud} acting on the d axis is obtained. Substituting $y = y_m$ into Eq. (24) the moment M_{ue} acting on the e-axis is obtained. Substituting $y = C_{y1} - L - e + c_3/2$ into Eq. (24) gives the moment M_{uf} acting on the f-axis.

The factored bending shear V_{uY} and the factored moment M_{uX} acting on the footing in the X axis for the interval $C_{y1} - a \leq y \leq C_{y1} - L - e$ is given by

$$V_{uY} = -\frac{M_{uxT}[ab_1 - C_{y1}(b_1 - b_2)](C_{y1}^2 - y^2)}{2I_x a} - \frac{M_{uxT}(b_1 - b_2)(C_{y1}^3 - y^3)}{3I_x a}$$
$$-\frac{R_u[ab_1 - C_{y1}(b_1 - b_2)](C_{y1} - y)}{Aa} - \frac{R_u(b_1 - b_2)(C_{y1}^2 - y^2)}{2Aa} + P_{u1} + P_{u2} \tag{25}$$

$$M_{uX} = \frac{M_{uxT}(b_1 - b_2)(y^4 - 2C_{y1}y^3 + 2C_{y1}^3 y - C_{y1}^4)}{12I_x a} + \frac{M_{uxT}[b_1(2C_{y1}^3 - 3C_{y1}^2 y + y^3)]}{6I_x}$$
$$-\frac{R_u(b_1 - b_2)(C_{y1} - y)^3}{6Aa} + \frac{R_u b_1(C_{y1} - y)^2}{2A} - R_u(C_{y1} - e - y) + P_{u2}L - M_{ux1} - M_{ux2} \tag{26}$$

where: the study width for the bending shear in the m axis is $w_m = b_1 - (L + e + c_3/2 + d)(b_1 - b_2)/a$, and the study width for the moment in the g axis is $w_g = b_1 - (L + e + c_3/2)(b_1 - b_2)/a$.

Now, substituting $y = C_{y1} - L - e - c_3/2 - d$ into Eq. (25) the bending shear V_{um} acting on the m axis is obtained. Substituting $y = C_{y1} - L - e - c_3/2$ into Eq. (26) gives the M_{ug} moment acting on the g axis.

2.3.2 Equations for punching shears

The factored punching shear for column 1 is presented in the perimeter formed by points 5, 6, 7 and 8, and for column 2 it is presented in the perimeter formed by points 9, 10, 11 and 12 according to the code ACI (see Fig. 5).

The punching shear that acts on the footing in column 1 V_{up1} and in column 2 V_{up2} are:

For edge column

$$V_{up1} = -\frac{M_{uxT}(4C_{y1} - 2c_1 - d)(2c_1 + d)(c_2 + d)}{8I_x}$$
$$-\frac{R_u(2c_1 + d)(c_2 + d)}{2A} + P_{u1} \tag{27}$$

For column without limit

$$V_{up1} = -\frac{[R_uI_x + M_{uxT}A(C_{y1} - e)](c_1 + d)(c_2 + d)}{AI_x}$$
$$+P_{u1} \tag{28}$$

For edge column

$$V_{up2} = \frac{M_{uxT}[4(L - C_{y1} + e) - d](2c_3 + d)(c_4 + d)}{8I_x}$$
$$-\frac{R_u(2c_3 + d)(c_4 + d)}{2A} + P_{u2} \tag{29}$$

For column without limit

$$V_{up2} = \frac{M_{uxT}(L - C_{y1} + e)(c_3 + d)(c_4 + d)}{I_x}$$
$$-\frac{R_u(c_3 + d)(c_4 + d)}{A} + P_{u2} \tag{30}$$

2.3.3 Equations of the construction code (ACI 318-14)

Equations according to the construction code for the moment in both axes are considered at the face of the column are (ACI 318-14 2014)

$$M_u = \emptyset_f b_w d^2 \rho f_y \left(1 - \frac{0.59A_sf_y}{b_w df'_c}\right) \tag{31}$$

$$\rho = \frac{A_s}{b_w d} \tag{32}$$

$$\rho_b = \frac{0.85\beta_1 f'_c}{f_y}\left(\frac{600}{600 + f_y}\right) \tag{33}$$

$$0.65 \leq \beta_1 = \left(1.05 - \frac{f'_c}{140}\right) \leq 0.85 \tag{34}$$

$$\rho_{max} = 0.75\rho_b \tag{35}$$

$$\rho_{min} = \begin{cases} \dfrac{0.25\sqrt{f'_c}}{f_y} \\ \dfrac{1.4}{f_y} \end{cases} \tag{36}$$
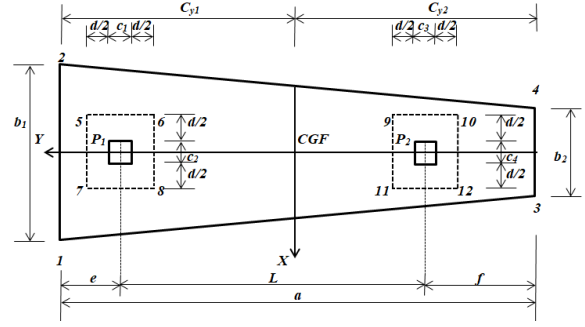

Fig. 5 Punching shears (Critical sections)

$$A_{st} = 0.0018b_w t \tag{37}$$

where: M_u = factored maximum moment, $\emptyset_f$ = factor of reduction of the resistance for bending and the value is 0.90, b_w = analysis width for structural member, ρ = relationship of A_s o bd, β_1 = factor that relates the depth of the equivalent rectangular compressive stress block to the depth of the neutral axis, f_y = specified yield strength of the reinforcing steel, f'_c = specified strength of the concrete to the compression to the 28 days, A_{st} = area of the reinforcing steel for temperature, t = total thickness of the footing.

Required strength U according to construction code to resist the moments and forces factored (moments and forces related internal) is (ACI 318-14 2014)

$$U = 12D + 1.6L \tag{38}$$

where: D = moments and forces factored due to dead loads, L = moments and forces factored due to live loads live loads.

Bending shear (unidirectional shear force) according construction code is presented at a distance "d" from the column face is (ACI 318-14 2014)

$$\emptyset_v V_{cf} \leq 0.17\emptyset_v\sqrt{f'_c}b_{ws}d \tag{39}$$

where: V_{cf} = bending shear that resist the concrete; $\emptyset_v$ = factor of reduction of the resistance for shear and the value is 0.85.

Punching shear (shear force bidirectional) construction code is presented at a distance "$d/2$" from the column face in both directions is shown (ACI 318-14 2014)

$$\emptyset_v V_{cp} = 0.17\emptyset_v\left(1 + \frac{2}{\beta_c}\right)\sqrt{f'_c}b_0d \tag{40a}$$

$$\emptyset_v V_{cp} = 0.083\emptyset_v\left(\frac{\alpha_s d}{b_0} + 2\right)\sqrt{f'_c}b_0d \tag{40b}$$

$$\emptyset_v V_{cp} = 0.33\emptyset_v\sqrt{f'_c}b_0d \tag{40c}$$

where: V_{cp} = punching shear that resist, β_c = relationship of long side between the short side of the column, b_0 = perimeter of the critical section, α_s is 40 for inner columns, 30 for edge columns, and 20 for corner columns. $\emptyset_v V_{cp}$ = largest value of the Equations (40a), (40b) and (40c). For

the boundary column $b_0 = 2c_1 + c_2 + 2d$, and for the inner column $b_0 = 2c_3 + 2c_4 + 4d$.

2.3.4 Objective function to minimum cost

The total cost "C_t" for a trapezoidal combined footing is

$$C_t = V_c C_c + V_s \gamma_s C_s \qquad (41)$$

where: C_c = cost of concrete for 1 m^3 of ready-mix reinforced concrete, C_s = cost of reinforcing steel for 1 kN of steel, V_s = volume of reinforcing steel, V_c = volume of concrete, and γ_s = steel density = 76.94 kN/m^3.

The volumes for trapezoidal combined footings are

$$V_s = \left(A_{syLT} + A_{syLB}\right)a + A_{sxTT}\left(\frac{b_1 + b_2}{2}\right) + A_{sxTB1}\left(\frac{b_1 + b_{11}}{2}\right) + A_{sP1}\left(\frac{b_{11} + b_{12}}{2}\right)$$
$$+ A_{sxTB2}\left(\frac{b_{12} + b_{21}}{2}\right) + A_{sP2}\left(\frac{b_{21} + b_{22}}{2}\right) + A_{sxTB3}\left(\frac{b_{22} + b_2}{2}\right) \qquad (42)$$

$$V_c = \frac{a(b_1 + b_2)t}{2} - \left(A_{syLT} + A_{syLB}\right)a - A_{sxTT}\left(\frac{b_1 + b_2}{2}\right) - A_{sxTB1}\left(\frac{b_1 + b_{11}}{2}\right)$$
$$- A_{sP1}\left(\frac{b_{11} + b_{12}}{2}\right) - A_{sxTB2}\left(\frac{b_{12} + b_{21}}{2}\right) - A_{sP2}\left(\frac{b_{21} + b_{22}}{2}\right) - A_{sxTB3}\left(\frac{b_{22} + b_2}{2}\right) \qquad (43)$$

where: t = total thickness of the footing, A_{syLT} = area of longitudinal reinforced steel at the top (direction of the "Y" axis), A_{syLB} = area of longitudinal reinforced steel in the bottom (direction of the "Y" axis), A_{sxTT} = area of reinforced steel at the top with a width a (direction of the "X" axis), A_{sP1} = area of reinforced steel at the bottom of the column 1 with a width w_1 (direction of the "X" axis), A_{sxTB1} = area of the transverse reinforcing steel at the bottom with a width ($e - w_1/2$) in the direction of the "X" axis, A_{sP2} = area of reinforced steel at the bottom of the column 2 with a width w_2 (direction of the "X" axis), A_{sxTB2} = area of the transverse reinforcing steel at the bottom with a width ($L - c_1/2 - c_3/2 - d$) in the direction of the "X" axis, A_{sxTB3} = area of the transverse reinforcing steel at the bottom with a width ($a - e - L - c_3/2 - d/2$) in the direction of the "X" axis.

Now, substituting Eqs. (42)-(43) into Eq. (41) is shown as follows

2.3.5 Constraint functions

The equations for the design of trapezoidal combined footings according to the ACI code are (ACI 318-14 2014): For the moments

$$|M_{ua}|, |M_{ub}|, |M_{uc}|, |M_{ud}|, |M_{ue}|, |M_{uf}|, |M_{ug}|$$
$$\leq \emptyset_f f_y d A_s \left(1 - \frac{0.59 A_s f_y}{b_w d f'_c}\right) \qquad (46)$$

where: the width of the study surface b_w for M_{ua} is w_1, for M_{ub} is w_2, for M_{uc} is w_c, for M_{ud} is w_d, for M_{ue} is w_e, for M_{uf} is w_f and for M_{ug} is w_g; the reinforcing steel areas As for M_{ua} is A_{sP1}, for M_{ub} is A_{sP2}, for M_{uc} is A_{syLBc}, for M_{ud} is A_{syLTd}, for

M_{ue} is A_{syLTe}, for M_{uf} is A_{syLTf}, and for M_{ug} is A_{syLBg}.

For the bending shear

$$|V_{uh}|, |V_{ui}|, |V_{uj}|, |V_{uk}|, |V_{ul}|, |V_{um}| \leq 0.17\emptyset_v\sqrt{f'_c}b_{ws}d \quad (47)$$

where: the width of the study surface b_{ws} for V_{uh} is w_1, for V_{ui} is w_2, for V_{uj} is w_j, for V_{uk} is w_k, for V_{ul} is w_l, and for V_{um} is w_m.

For the punching shear

$$|V_{up1}|, |V_{up2}| \leq \begin{cases} 0.17\emptyset_v\left(1 + \frac{2}{\beta_c}\right)\sqrt{f'_c}b_0 d \\ 0.083\emptyset_v\left(\frac{\alpha_s d}{b_0} + 2\right)\sqrt{f'_c}b_0 d \\ 0.33\emptyset_v\sqrt{f'_c}b_0 d \end{cases} \qquad (48)$$

$$C_t = C_c \left[\frac{a(b_1 + b_2)t}{2} - \left(A_{syLT} + A_{syLB}\right)a - A_{sxTT}\left(\frac{b_1 + b_2}{2}\right) - A_{sxTB1}\left(\frac{b_1 + b_{11}}{2}\right) - A_{sP1}\left(\frac{b_{11} + b_{12}}{2}\right)\right.$$
$$\left. - A_{sxTB2}\left(\frac{b_{12} + b_{21}}{2}\right) - A_{sP2}\left(\frac{b_{21} + b_{22}}{2}\right) - A_{sxTB3}\left(\frac{b_{22} + b_2}{2}\right)\right]$$
$$+ \gamma_s C_s \left[\left(A_{syLT} + A_{syLB}\right)a + A_{sxTT}\left(\frac{b_1 + b_2}{2}\right) + A_{sxTB1}\left(\frac{b_1 + b_{11}}{2}\right) + A_{sP1}\left(\frac{b_{11} + b_{12}}{2}\right) + A_{sxTB2}\left(\frac{b_{12} + b_{21}}{2}\right)\right.$$
$$\left. + A_{sP2}\left(\frac{b_{21} + b_{22}}{2}\right) + A_{sxTB3}\left(\frac{b_{22} + b_2}{2}\right)\right] \qquad (44)$$

Subsequently, substituting $\alpha = \gamma_s C_s/C_c \rightarrow \gamma_s C_s = \alpha C_c$ into Eq. (44) is presented by the following equation

where: β_c is the ratio of the long side between the short side of column, $\alpha_s = 20$ for corner columns, αs = 30 for edge

$$C_t = C_c \left\{\left[\left(A_{syLT} + A_{syLB}\right)a + A_{sxTT}\left(\frac{b_1 + b_2}{2}\right) + A_{sxTB1}\left(\frac{b_1 + b_{11}}{2}\right) + A_{sP1}\left(\frac{b_{11} + b_{12}}{2}\right) + A_{sxTB2}\left(\frac{b_{12} + b_{21}}{2}\right)\right.\right.$$
$$\left.\left. + A_{sP2}\left(\frac{b_{21} + b_{22}}{2}\right) + A_{sxTB3}\left(\frac{b_{22} + b_2}{2}\right)\right](\alpha - 1) + \frac{a(b_1 + b_2)(d + r)}{2}\right\} \qquad (45)$$

columns, and $\alpha_s = 40$ for interior columns, the perimeter of the critical section for column 1 is: $b_0 = 2c_1 + c_2 + 2d$ (edge column) and $b_0 = 2c_1 + 2c_2 + 4d$ (column without limit), for column 2 is: $b_0 = 2c_3 + c_4 + 2d$ (edge column) and $b_0 = 2c_3 + 2c_4 + 4d$ (column without limit).

For the maximum and minimum percentage of reinforcing steel

$$\rho_{P_1}, \rho_{P_2}, \rho_{yLBc}, \rho_{yLTd}, \rho_{yLTe}, \rho_{yLTf}, \rho_{yLBg} \leq \rho_{max} = 0.75\left[\frac{0.85\beta_1 f'_c}{f_y}\left(\frac{600}{600 + f_y}\right)\right] \tag{49}$$

$$\rho_{P_1}, \rho_{P_2}, \rho_{yLBc}, \rho_{yLTd}, \rho_{yLTe}, \rho_{yLTf}, \rho_{yLBg} \geq \rho_{min} = \begin{cases} \dfrac{0.25\sqrt{f'_c}}{f_y} \\ \dfrac{1.4}{f_y} \end{cases} \tag{50}$$

For the area of reinforcement steel

$$A_{sP1} = \rho_{P1} w_1 d \tag{51}$$

$$A_{sP2} = \rho_{P2} w_2 d \tag{52}$$

$$A_{syLBc} = \rho_{yLBc} w_c d \tag{53}$$

$$A_{syLTd} = \rho_{yLTd} w_d d \tag{54}$$

$$A_{syLTe} = \rho_{yLTe} w_e d \tag{55}$$

$$A_{syLTf} = \rho_{yLTf} w_f d \tag{56}$$

$$A_{syLBg} = \rho_{yLBg} w_g d \tag{57}$$

$$A_{sxTT} = 0.0018 a d \tag{58}$$

$$A_{sxTB1} = 0.0018(e - c_1/2 - d/2)d \tag{59}$$

$$A_{sxTB2} = 0.0018(L - c_1/2 - c_3/2 - d)d \tag{60}$$

$$A_{sxTB2} = 0.0018(L - c_1/2 - c_3/2 - d)d \tag{61}$$

$$A_{syLT} \geq \begin{cases} \dfrac{A_{syLTd}(b_1 + b_2)}{2w_d} \\ \dfrac{A_{syLTe}(b_1 + b_2)}{2w_e} \\ \dfrac{A_{syLTf}(b_1 + b_2)}{2w_f} \end{cases} \tag{62}$$
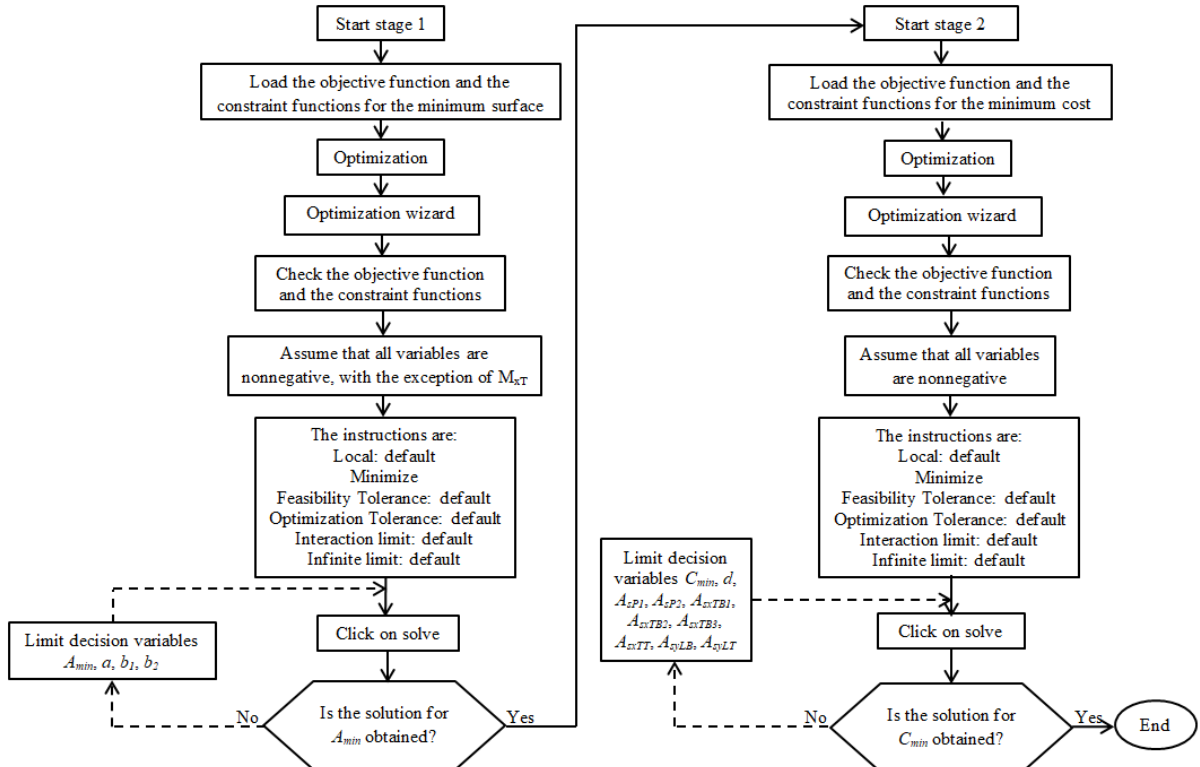

Fig. 6 Flow chart by Maple software for minimum cost of trapezoidal combined footings

Table 1 Constraint functions for the trapezoidal combined footings

Case	Constraint functions and conditions
1	Eqs. (3) to (13), $a \geq 0$, $b_1 = 3$ and $b_2 = 2$
2	Eqs. (3) to (12) (14), $a \geq 0$, $b_1 \geq 0$ and $b_2 \geq 0$
3	Eqs. (3) to (12) (15), $a \geq 0$, $b_1 \geq 0$ and $b_2 \geq 0$
4	Eqs. (3) to (12) (16), $a \geq 0$, $b_1 \geq 0$ and $b_2 \geq 0$

*where: a, b_1, b_2 in m

$$A_{syLB} \geq \begin{cases} \dfrac{A_{syLBc}(b_1 + b_2)}{2w_c} \\ \dfrac{A_{syLBg}(b_1 + b_2)}{2w_g} \end{cases} \quad (63)$$

Fig. 6 presents the flowchart to obtain the minimum cost for a reinforced concrete trapezoidal combined footing using Maple software.

Table 1 shows the constraint functions and the conditions that are taken into account for the four cases.

Subsequently, the proposed dimensions are adjusted according to the initial solution to obtain the practical solution.

The factored loads and moments acting on the trapezoidal combined footing due to the columns are: $P_{u1} = 1680\ kN$, $M_{ux1} = 328\ kN\text{-}m$, $M_{uy1} = 408\ kN\text{-}m$, $P_{u2} = 1400\ kN$, $M_{ux2} = 272\ kN\text{-}m$, $M_{uy2} = 360\ kN\text{-}m$.

Now, substituting the corresponding values into Eq. (45) to obtain the objective function (optimal design or minimum cost), and also into Eqs. (46) to (63) to find the constraint functions and an initial solution are obtained.

Subsequently, the proposed effective depth is adjusted according to the initial solution to obtain the practical

solution. The effective depth adjusted for case 1 is $d = 42.00\ cm$, for case 2 is $d = 52.00\ cm$, for case 3 is $d = 47.00\ cm$, for case 4 is $d = 92.00\ cm$.

The minimum area and the minimum cost are obtained by MAPLE-15 software for the reinforced concrete trapezoidal combined footings.

Fig. 7 shows the optimal areas for the four cases, where the initial solution (IS) and practical solution (PS) is presented. The initial solution is generated with the constant (known) parameters that are: P_1, M_{x1}, M_{y1}, P_2, M_{x2}, M_{y2}, R, c_1, c_2, c_3, c_4, L, q_{aa}. The practical solution is obtained from the dimensions of the initial solution, these are set to values closer and greater than 0.05 or 0.10 and checked, and the same optimal area equations are used.

Fig. 8 shows the optimal costs for the four cases, where the initial solution and practical solution are presented. The initial solution is generated with the constant (known) parameters that are: a, b_1, b_2, e, f, M_{uc}, M_u, M_{ue}, M_{uf} and M_{ug}, and the parameters M_{ua}, M_{ub}, V_{uh}, V_{ui}, V_{uj}, V_{uk}, V_{ul}, V_{um}, V_{up1} and V_{up2} are presented in function of d. The practical solution is obtained from the effective depth of the initial solution; these are set to values closer and greater taking into account the full thickness of footing and checked, and the same optimal cost equations are used.

4. Results

Fig. 7 shows the optimal solution to obtain the minimum area of the four cases. The results present the following: 1) The smallest dimension in the Y direction appears in cases 3 and 4 of $a = 5.40\ m$ (IS and PS), and the largest occurs in case 1 of $a = 6.53\ m$ (IS) and $a = 6.60\ m$ (PS); 2) The smallest dimension b_1 in the X direction appears in case 1 of $b_1 = 3.00\ m$ (IS and PS), and the largest occurs in case 2 of $b_1 = 4.75$ m (IS) and $b_1 = 4.80$ m (PS); 3) The smallest
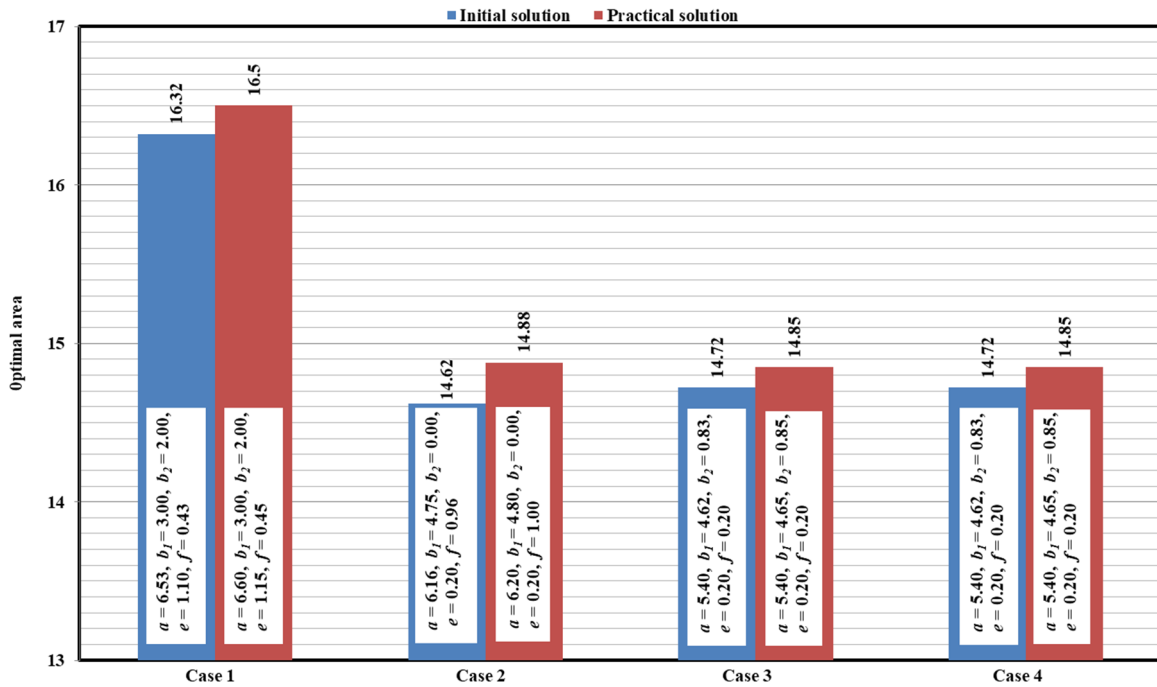

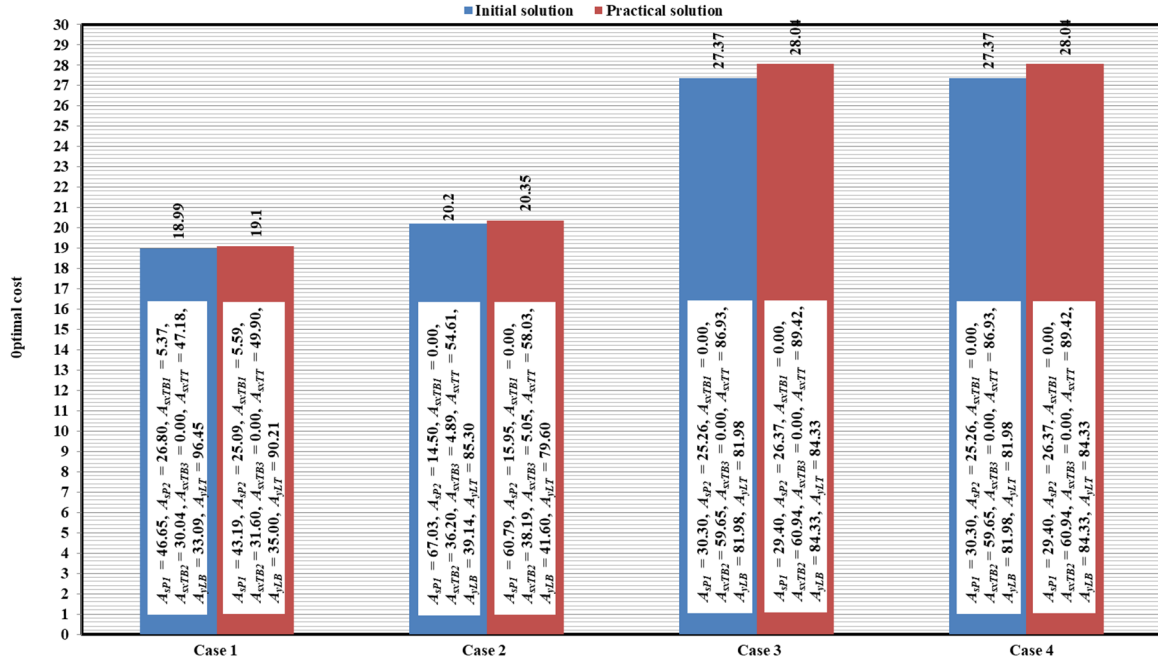Fig. 7 Optimal areas for the trapezoidal combined footings (Optimal area in m^2, footing dimensions in m)

Fig. 8 Optimal costs for the trapezoidal combined footings (Optimal cost in function of C_c (concrete cost), the areas of reinforced steel in cm^2)

dimension b_2 in the X direction appears in case 2 of $b_2 = 0.00$ m (IS and PS), and the largest occurs in case 1 of $b_2 = 2.00$ m (IS and PS); 4) The smallest distance in the Y direction from the center of column 1 to the free end appears in cases 2, 3 and 4 of $e = 0.20$ m (IS and PS), and the largest occurs in case 1 of $e = 1.10$ m (IS) and $e = 1.15$ m (PS); 5) The smallest distance in the Y direction from the center of column 2 to the free end appears in cases 3 and 4 of $f = 0.20$ m (IS and PS), and the largest occurs in case 2 of $f = 0.96$ m (IS) and $f = 1.00$ m (PS); 6) The smallest area occurs in case 2 of $A_{min} = 14.62$ m^2 (IS) and in cases 3 and 4 of $A_{min} = 14.72$ m^2 (PS), and the largest area occurs in case 1 of $A_{min} = 16.32$ m^2 (IS) and $A_{min} = 16.50$ m^2 (PS).

Fig. 8 shows the optimal solution to obtain the minimum cost of the four cases. The initial solution is obtained from the dimensions of the footing of the practical solution as shown in Fig. 7, and later the effective depth is adjusted to obtain the practical solution. The results show the following: 1) The smallest reinforcing steel area at the bottom of column 1 in the X-axis direction occurs in cases 3 and 4 $A_{sp1} = 30.30$ cm^2 (IS) and $A_{sp1} = 29.40$ cm^2 (PS), and the largest area occurs in case 2 of $A_{sp1} = 67.03$ cm^2 (IS) and $A_{sp1} = 60.79$ cm^2 (PS); 2) The smallest reinforcing steel area at the bottom of column 2 in the X-axis direction occurs in case 2 $A_{sp2} = 14.50$ cm^2 (IS) and $A_{sp2} = 15.95$ cm^2 (PS), and the largest area occurs in case 1 of $A_{sp2} = 26.80$ cm^2 (IS) and in cases 3 and 4 $A_{sp2} = 26.37$ cm^2 (PS); 3) The smallest reinforcing steel area at the bottom with width ($e - w_1/2$) in the X-direction occurs in cases 2, 3 and 4 of $A_{sxTB1} = 0$ cm^2 (IS and PS) because the width is zero, and the largest area occurs in case 1 of $A_{sxTB1} = 5.37$ cm^2 (IS) and $A_{sxTB1} = 5.59$ cm^2 (PS); 4) The smallest reinforcing steel area at the bottom with width ($L - c_1/2 - c_3/2 - d$) in the X-direction occurs in case 1 of $A_{sxTB2} = 30.04$ cm^2 (IS) and $A_{sxTB2} = 31.60$ cm^2 (PS), and the largest area occurs in cases 3 and 4
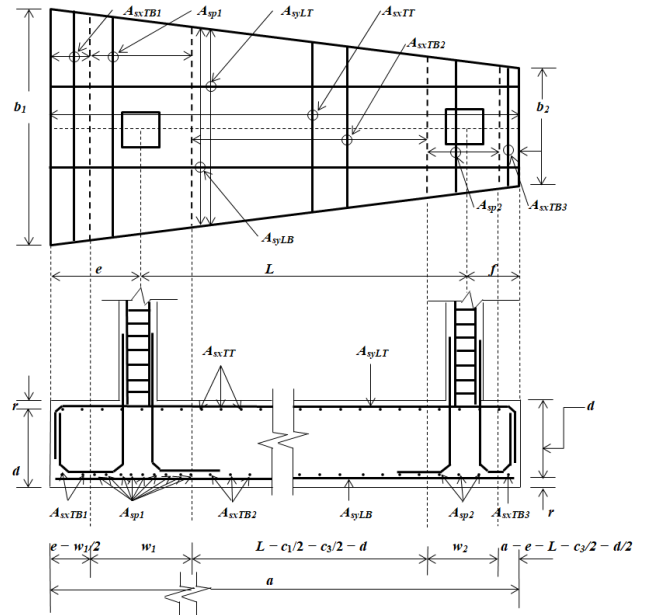

Fig. 9 Diagram for the trapezoidal combined footings

of $A_{sxTB2} = 59.65$ cm^2 (IS) and $A_{sxTB2} = 60.94$ cm^2 (PS); 5) The smallest reinforcing steel area at the bottom with width ($a - e - L - c_3/2 - d/2$) in the X-direction occurs in cases 1, 3 and 4 of $A_{sxTB3} = 0$ cm^2 (IS and PS), and the largest area occurs in case 2 of $A_{sxTB3} = 4.89$ cm^2 (IS) and $A_{sxTB3} = 5.05$ cm^2 (PS); 6) The smallest reinforcing steel area at the top with a width a in the X-direction occurs in case 1 of $A_{sxTT} = 47.18$ cm^2 (IS) and $A_{sxTT} = 49.90$ cm^2 (PS), and the largest area occurs in cases 3 and 4 of $A_{sxTT} = 86.93$ cm^2 (IS) and $A_{sxTT} = 89.42$ cm^2 (PS); 7) The smallest reinforcing steel area at the bottom located in the middle part in the Y-axis

direction occurs in case 1 of A_{syLB} = 33.09 cm^2 (IS) and A_{syLB} = 35.00 cm^2 (PS), and the largest area occurs in cases 3 and 4 of A_{syLB} = 81.98 cm^2 (IS) and A_{syLB} = 84.33 cm^2 (PS); 8) The smallest reinforcing steel area in the upper part located in the middle part in the Y-axis direction occurs in cases 3 and 4 of A_{syLT} = 81.98 cm^2 (IS) and in case 2 of A_{syLT} = 79.60 cm^2 (PS), and the largest area occurs in case 1 of A_{syLT} = 96.45 cm^2 (IS) and A_{syLT} = 90.21 cm^2 (PS); 9) The lowest cost occurs in case 1 of C_{min} = 18.99C_c (IS) and C_{min} = 19.10C_c (PS), and the highest cost occurs in cases 3 and 4 of C_{min} = 27.37C_c (IS) and C_{min} = 28.04C_c (PS).

The results proposed in Fig. 8 must adjust to the reinforcing steel areas to the standard measurements of the rods to obtain the final design.

Fig. 9 shows in detail the final design under the minimum cost criteria in general.

5. Conclusions

Foundation of a structure is the essential part to transmit the column or wall loads to the underlying ground below the structure. The novel model proposed in this article generates results that have an unparalleled accuracy for all foundation engineering problems. The main part of this research is to obtain the optimal design (reinforcing steel and thickness of the trapezoidal combined footings) using the optimization techniques.

The proposed model presented in this article can be applied to the following types:

1) Footings under concentric load in each column.
2) Footings under concentric load and moment in a direction in each column.
3) Footings under concentric load and moments in both directions in each column.

The main advantages of these models are:

1. The methodology shown in this paper is more accurate and converges more quickly.
2. The classical model will not be practical compared to this methodology; because the classical model takes into account only the greater pressure applied throughout the contact surface of the footing (pressure is equal in all points of the footing).
3. The new models can be used to obtain the minimum area and minimum cost for the design of rectangular combined footings for the four cases, substituting $b_1 = b_2$ in the two models.
4. The optimal model for the minimum area presented in this document is more general because it considers the four cases, and Pasillas-Orona *et al.* (2020) takes into account only two cases (Case 2: with a limit in column 1, and Case 4: with two limited opposite sides).
5. The optimal model for the design of trapezoidal combined footings are more general because it consider the four cases, and Luévanos-Rojas (2015a) shows a mathematical model for the design of boundary trapezoidal combined footings to obtain the thickness and reinforcing steel areas of trapezoidal combined footings for one case (Case 2: the footing is limited to one line property on the side of the heavier load).
6. The optimal models for minimum area and minimum cost for the design of trapezoidal combined footings could be used for different reinforced concrete design codes, simply by modifying the resisting capacity equations for moment, for bending shear, and for the punching shear, according to each code.

Therefore, the model presented in this article to obtain the optimal design (minimum cost) can be applied to the combined footings (rectangular and trapezoidal), this study assumes that soil support layers are elastic and the rigid footing, which comply with the biaxial bending equation, i.e., the pressure diagram presents a linear variation.

Suggestions for next investigations can be: if there is another type of soil, such as totally clayey soils (cohesive soils) or totally sandy soils (granular soils), the pressure diagram should be considered differently because it is not linear.

References

ACI 318-14 (2014), Building Code Requirements for Structural Concrete and Commentary; Committee 318, New York: American Concrete Institute.

Agrawal, R. and Hora, M.S. (2012), "Nonlinear interaction behaviour of infilled frame-isolated footings-soil system subjected to seismic loading", *Struct. Eng. Mech., Int. J.*, **44**(1), 85-107. https://doi.org/10.12989/sem.2012.44.1.085

Al-Ansari, M.S. (2013), "Structural cost of optimized reinforced concrete isolated footing", *Int. Scholar. Scientif. Res. Innov.*, **7**(4), 193-200.
https://zenodo.org/record/1080444#.Xkth1GhKiUk

Al-Ansari, M.S. (2014), "Cost of reinforced concrete paraboloid shell footing", *Int. J. Struct. Analys. Des.*, **1**(3), 111-119.
http://journals.theired.org/assets/pdf/20141006_094159.pdf

Alazwari, M.A., Daikh, A.A., Houari, M.S.A., Tounsi, A. and Eltaher, M.A. (2021), "On static buckling of multilayered carbon nanotubes reinforced composite nanobeams supported on non-linear elastic foundations", *Steel Compos. Struct., Int. J.*, **40**(3), 389-404. https://doi.org/10.12989/scs.2021.40.3.389

Alijani, M. and Bidgoli, M.R. (2018), "Agglomerated SiO2 nanoparticles reinforced-concrete foundations based on higher order shear deformation theory: Vibration analysis", *Adv. Concrete Constr., Int. J.*, **6**(6), 585-610.
https://doi.org/10.12989/acc.2018.6.6.585

Anil, Ö, Akbaş, S.O., Babagĺray, S., Gel, A.C. and Durucan, C. (2017), "Experimental and finite element analyses of footings of varying shapes on sand", *Geomech. Eng., Int. J.*, **12**(2), 223-238. https://doi.org/10.12989/gae.2017.12.2.223

Basudhar, P.K., Dey, A. and Mondal, A.S. (2012), "Optimal Cost-Analysis and Design of Circular Footings", *Int. J. Eng. Technol. Innov.*, **2**(4), 243-264.
https://pdfs.semanticscholar.org/158d/d842b78d4efdf970070d3 4e94b34645a68ec.pdf

Bensaid, I. and Kerboua, B. (2019), "Improvement of thermal buckling response of FG-CNT reinforced composite beams with temperature-dependent material properties resting on elastic foundations", *Adv. Aircr. Spacecr. Sci., Int. J.*, **6**(3), 207-223.
https://doi.org/10.12989/aas.2019.6.3.207

Chaudhuri, P. and Maity, D. (2020), "Cost optimization of rectangular RC footing using GA and UPSO", *Soft Computing*, **24**, 709-721.

https://link.springer.com/article/10.1007/s00500-019-04437-x

Chen, W-R., Chen, C-S and Yu, S-Y. (2011), "Nonlinear vibration of hybrid composite plates on elastic foundations", *Struct. Eng. Mech., Int. J.*, **37**(4), 367-383. https://doi.org/10.12989/sem.2011.37.4.367

Dezhkam, B. and Yaghfoori, A. (2018), "Soil foundation effect on the vibration response of concrete foundations using mathematical model", *Comput. Concrete, Int. J.*, **22**(2), 221-225. https://doi.org/10.12989/cac.2018.22.2.221

Garay-Gallegos, J.R., Luévanos-Rojas, A., López-Chavarría, S., Medina-Elizondo, M., Aguilera-Mancilla, G. and García-Canales, E. (2022), "A comparative study between the new model and the current model for T-shaped combined footings", *Geomech. Eng., Int. J.*, **30**(6), 525-538. https://doi.org/10.12989/gae.2022.30.6.525

García-Galván, M., Luévanos-Rojas, A., López-Chavarría, S., Medina-Elizondo, M. and Rivera-Mendoza, J.B. (2022), "A comparative study between trapezoidal combined footings and T-shaped combined footings", *Coupled Syst. Mech., Int. J.*, **11**(3), 233-257. https://doi.org/10.12989/csm.2022.11.3.233

Gör, M. (2022), "Analyzing the bearing capacity of shallow foundations on two-layered soil using two novel cosmology-based optimization techniques", *Smart Struct. Syst., Int. J.*, **29**(3), 513-522. https://doi.org/10.12989/sss.2022.29.3.513

Guler, K. and Celep, Z. (2005), "Response of a rectangular plate-column system on a tensionless Winkler foundation subjected to static and dynamic loads", *Struct. Eng. Mech., Int. J.*, **21**(6), 699-712. https://doi.org/10.12989/sem.2005.21.6.699

Hassaan, G.A. (2014), "Optimal design of machinery shallow foundations with sand soils", *Int. J. Res. Eng. Technol.*, **3**(5), 1-8. https://scholar.cu.edu.eg/?q=galal/files/founddesign_sand.pdf

Himeur, N., Mamen, B., Benguediab, S., Bouhadra, A., Menasria, A., Bouchouicha, B., Bourada, F., Benguediab, M. and Tounsi, A. (2022), "Coupled effect of variable Winkler–Pasternak foundations on bending behavior of FG plates exposed to several types of loading", *Steel Compos. Struct., Int. J.*, **44**(3), 353-369. https://doi.org/10.12989/scs.2022.44.3.353

Jelusic, P. and Zlender, B. (2018), "Optimal design of pad footing based on MINLP optimization", *Soils Found.*, 58(2), 277-289. https://doi.org/10.1016/j.sandf.2018.02.002

Kalinli, A., Acar, C. and Gündüz, Z. (2011), "New approaches to determine the ultimate bearing capacity of shallow foundations based on artificial neural networks and antcolony optimization", *Eng. Geol.*, **117**(1-2), 29-38. https://doi.org/10.1016/j.enggeo.2010.10.002

Kashani, A.R., Camp, C.V., Akhani, M. and Ebrahimi, S. (2022), "Optimum design of combined footings using swarm intelligence-based algorithms", *Adv. Eng. Softw.*, **169**, 103140. https://doi.org/10.1016/j.advengsoft.2022.103140

Keawsawasvong, S. and Ukritchon, B. (2016), "A Practical Method for the Optimal Design of Continuous Footing Using Ant-Colony Optimization", *Acta Geotech. Slov.*, **13**(2), 45-55. https://dk.um.si/IzpisGradiva.php?id=70877

Khajehzadeh, M., Taha, M.R., El-Shafie, A. and Eslami, M. (2012), "Optimization of shallow foundation using gravitational search algorithm", *Res. J. Appl. Sci. Eng. Technol.*, **4**(9),1124-1130. https://ukm.pure.elsevier.com/en/publications/optimization-of-shallow-foundation-using-gravitational-search-alg

Khajehzadeh, M., Taha, M.R. and Eslami, M. (2014), "Multi-objective optimization of foundation using global-local gravitational search algorithm", *Struct. Eng. Mech., Int. J.*, **50**(3), 257-273. https://doi.org/10.12989/sem.2014.50.3.257

Khatri, V.N., Debbarma, S.P., Dutta, R.K. and Mohanty, B. (2017), "Pressure-settlement behavior of square and rectangular skirted footings resting on sand", *Geomech. Eng., Int. J.*, **12**(4), 689-705. https://doi.org/10.12989/gae.2017.12.4.689

Lezgy-Nazargah, M., Mamazizi, A. and Khosravi, H. (2022), "Analysis of shallow footings rested on tensionless foundations using a mixed finite element model", *Struct. Eng. Mech., Int. J.*, **81**(3), 379-394. https://doi.org/10.12989/sem.2022.81.3.379

Lins da Silva, J., Aoki, N. and Barbosa Franco, Y. (2017), "Use of the order statistics when predicting pile foundation failure probability", *Dyn.*, **84**(200), 247-252. http://dx.doi.org/10.15446/dyna.v84n200.54867

López-Chavarría, S., Luévanos-Rojas, A. and Medina-Elizondo, M. (2017), "A new mathematical model for design of square isolated footings for general case", *Int. J. Innov. Comput. I.*, **13**(4), 1149-1168. http://www.ijicic.org/ijicic-130406.pdf

López-Chavarría, S., Luévanos-Rojas, A., Medina-Elizondo, M., Sandoval-Rivas, R. and Velázquez-Santillán, F. (2019), "Optimal design for the reinforced concrete circular isolated footings", *Adv. Comput. Des., Int. J.*, **4**(3), 169-183. https://doi.org/10.12989/acd.2019.4.3.273

Lu, X. and Aboutaha, R.S. (2021), "Strengthening of isolated square FOOTINGS using passive wrapping systems", *Comput. Concrete.*, **27**(1), 41-54. https://doi.org/10.12989/cac.2021.27.1.041

Luévanos-Rojas, A. (2014a), "Design of isolated footings of circular form using a new model", *Struct. Eng. Mech., Int. J.*, **52**(4), 767-786. http://dx.doi.org/10.12989/sem.2014.52.4.767

Luévanos-Rojas, A. (2014b), "Design of boundary combined footings of rectangular shape using a new model", *Dyn.*, **81**(188), 199-208. http://dx.doi.org/10.15446/dyna.v81n188.41800

Luévanos-Rojas, A. (2015a), "Design of boundary combined footings of trapezoidal form using a new model", *Struct. Eng. Mech., Int. J.*, **56**(5), 745-765. https://doi.org/10.12989/sem.2015.56.5.745

Luévanos-Rojas, A. (2015b), "A new mathematical model for dimensioning of the boundary trapezoidal combined footings", *Int. J. Innov. Comput. I.*, **11**(4), 1269-1279. http://www.ijicic.org/ijicic-110411.pdf

Luévanos-Rojas, A. (2016a), "A comparative study for the design of rectangular and circular isolated footings using new models", *Dyn.*, **83**(196), 149-158. http://dx.doi.org/10.15446/dyna.v83n196.51056

Luévanos-Rojas, A. (2016b), "A new model for the design of rectangular combined boundary footings with two restricted opposite sides", *Alconpat Journal*, **6**(2), 172-187. http://dx.doi.org/10.21041/ra.v6i2.137

Luévanos-Rojas, A., Faudoa-Herrera, J.G., Andrade-Vallejo, R.A. and Cano-Alvarez, M.A. (2013), "Design of isolated footings of rectangular form using a new model", *Int. J. Innov. Comput. I.*, 9(10), 4001-4022. http://www.ijicic.org/ijicic-12-10031.pdf

Luévanos-Rojas, A., López-Chavarría, S. and Medina-Elizondo, M. (2017a), "Optimal design for rectangular isolated footings using the real soil pressure", *Ing. Invest.*, **37**(2), 25-33. http://dx.doi.org/10.15446/ing.investig.v37n2.61447

Luévanos-Rojas, A., Barquero-Cabrero, J.D., López-Chavarría, S. and Medina-Elizondo, M. (2017b), "A comparative study for design of boundary combined footings of trapezoidal and rectangular forms using new models", *Coupled Syst. Mech., Int. J.*, **6**(4), 417-437. https://doi.org/10.12989/csm.2017.6.4.417

Luévanos-Rojas, A., López-Chavarría, S. and Medina-Elizondo, M. (2018), "A new model for T-shaped combined footings Part II: Mathematical model for design", *Geomech. Eng., Int. J.*, **14**(1), 61-69. https://doi.org/10.12989/gae.2018.14.1.061

Maheshwari, P. and Khatri, S. (2012), "Influence of inclusion of geosynthetic layer on response of combined footings on stone column reinforced earth beds", *Geomech. Eng., Int. J.*, **4**(4), 263-279. https://doi.org/10.12989/gae.2012.4.4.263

Malapur, M.M., Cholappanavar, P. and Fernandes, R.J. (2018), "Optimization of RC column and footings using genetic

algorithm", *Int. Res. J. Eng. Technol.* (*IRJET*), **5**(8), 546-552. https://www.irjet.net/archives/V5/i8/IRJET-V5I897.pdf

Mohamed, F.M.O., Vanapalli, S.K. and Saatcioglu, M. (2013), "Generalized Schmertmann Equation for settlement estimation of shallow footings in saturated and unsaturated sands", *Geomech. Eng., Int. J.*, **5**(4), 363-377. https://doi.org/10.12989/gae.2013.5.4.343

Mohebkhah, A. (2017), "Bearing capacity of stripfootingson a stone masonry trench in clay", *Geomech. Eng., Int. J.*, **13**(2), 255-267. https://doi.org/10.12989/gae.2017.13.2.255

Orbanich, C.J. and Ortega, N.F. (2013), "Analysis of elastic foundation plates with internal and perimetric stiffening beams on elastic foundations by using Finite Differences Method", *Struct. Eng. Mech., Int. J.*, **45**(2), 169-182. https://doi.org/10.12989/sem.2013.45.2.169

Orbanich, C.J., Dominguez, P.N. and Ortega, N.F. (2012), "Strenghtening and repair of concrete foundation beams whit fiber composite materials", *Mater. Struct.*, **45**(11), 1693-1704. https://doi.org/10.1617/s11527-012-9866-6

Pasillas-Orona, A.I., Luévanos-Rojas, A., López-Chavarría, S., Medina-Elizondo, M. and Aguilera-Mancilla, G. (2020), "Un modelo optimizado para zapatas combinadas trapezoidales apoyadas sobre el terreno: Superficie óptima", *Acta Universitaria*, **30**, e2973. http://doi.org/10.15174.au.2020.2973

Rad, A.B. (2012), "Static response of 2-D functionally graded circular plate with gradient thickness and elastic foundations to compound loads", *Struct. Eng. Mech., Int. J.*, **44**(2), 139-161. https://doi.org/10.12989/sem.2012.44.2.139

Rawat, S. and Mittal, R.K. (2018),"Optimization of Eccentrically Loaded Reinforced-Concrete Isolated Footings", *Practice Period. Struct. Des. Constr.*, **23**(2). https://doi.org/10.1061/(ASCE)SC.1943-5576.0000366

Rizwan, M., Alam, B., Rehman, F.U., Masud, N., Shahzada, K., Masud, T. (2012), "Cost Optimization of Combined Footings Using Modified Complex Method of Box", *Int. J. Adv. Struct. Geotech. Eng.*, **1**(1), 24-28. https://www.academia.edu/20635751/Cost_Optimization_of_Combined_Footings_Using_Modified_Complex_Method_of_Box

Shahin, M.A. and Cheung, E.M. (2011), "Stochastic design charts for bearing capacity of strip footings", *Geomech. Eng., Int. J.*, **3**(2), 153-167. https://doi.org/10.12989/gae.2011.3.2.153

Smith-Pardo, J.P. (2011), "Performance-based framework for soil-structure systems using simplified rocking foundation models", *Struct. Eng. Mech., Int. J.*, **40**(6), 763-782. https://doi.org/10.12989/sem.2011.40.6.763

Soltani, K., Bessaim, A., Houari, M.S.A., Kaci, A., Benguediab, M., Tounsi, A. and Alhodaly, M.S. (2019), "A novel hyperbolic shear deformation theory for the mechanical buckling analysis of advanced composite plates resting on elastic foundations", *Steel Compos. Struct., Int. J.*, **30**(1), 13-29. https://doi.org/10.12989/scs.2019.30.1.013

Turedi, Y., Emirler, B., Ornek, M. and Yildiz, A. (2019), "Determination of the bearing capacity of model ring footings: Experimental and numerical investigations", *Geomech. Eng., Int. J.*, **18**(1), 29-39. https://doi.org/10.12989/gae.2019.18.1.029

Uncuoğlu, E. (2015), "The bearing capacity of square footings on a sand layer overlying clay", *Geomech. Eng., Int. J.*, **9**(3), 287-311. https://doi.org/10.12989/gae.2015.9.3.287

Velázquez-Santillán, F., Luévanos-Rojas, A., López-Chavarría, S., Medina-Elizondo, M. and Sandoval-Rivas, R. (2018), "Numerical experimentation for the optimal design for reinforced concrete rectangular combined footings", *Adv. Comput. Des., Int. J.*, **3**(1), 49-69. https://doi.org/10.12989/acd.2018.3.1.049

Wang, Y. (2009), "Reliability-based economic design optimization of spread foundations", *J. Geotech. Geoenviron.*, **135**(7), 954-959. https://doi.org/10.1061/(ASCE)GT.1943-5606.0000013

Wang, Y. and Kulhawy, F.H. (2008), "Economic Design Optimization of Foundation", *J. Geotech. Geoenviron.*, **134**(8), 1097-1105. https://doi.org/10.1061/(ASCE)1090-0241(2008)134:8(1097)

Yáñez-Palafox, J.A., Luévanos-Rojas, A., López-Chavarría, S. and Medina-Elizondo, M. (2019), "Modeling for the strap combined footings Part II: Mathematical model for design", *Steel Compos. Struct., Int. J.*, **30**(2), 109-121. https://doi.org/10.12989/scs.2019.30.2.109

Yeh, J.-P. and Huang, K.-H. (2016), "Application of Genetic Algorithms Coupled with Neural Networks to Optimization of Reinforced Concrete Footings", *Transact. Mach. Learn. Artif. Intell.*, **4**(4), 18-35. https://journals.scholarpublishing.org/index.php/TMLAI/article/view/2150

Yeh, J.-P. and Huang, K.-H. (2017), "Effects of Strengths of Steel and Concrete, Eccentricity and Bar Size on the Optimization of Eccentrically Loaded Footings", *Transact. Mach. Learn. Artif. Intell.*, **5**(5), 87-97. https://journals.scholarpublishing.org/index.php/TMLAI/issue/view/169/218

Zhang, L., Zhao, M.H., Xiao, Y. and Ma, B.H. (2011), "Nonlinear analysis of finite beam resting on Winkler with consideration of beam-soil interface resistance effect", *Struct. Eng. Mech., Int. J.*, **38**(5), 573-592. https://doi.org/10.12989/sem.2011.38.5.573

CC